# Casein kinase 1 and disordered clock proteins form functionally equivalent, phospho-based circadian modules in fungi and mammals

Daniela Marzoll[a] , Fidel E. Serrano[a] , Anton Shostak[a], Carolin Schunke[a] , Axel C. R. Diernfellner[a], and Michael Brunner[a,1]

[a]Biochemistry Centre, Heidelberg University, 69120 Heidelberg, Germany

**Circadian clocks are timing systems that rhythmically adjust physiology and metabolism to the 24-h day–night cycle. Eukaryotic circadian clocks are based on transcriptional–translational feedback loops (TTFLs). Yet TTFL-core components such as Frequency (FRQ) in *Neurospora* and Periods (PERs) in animals are not conserved, leaving unclear how a 24-h period is measured on the molecular level. Here, we show that CK1 is sufficient to promote FRQ and mouse PER2 (mPER2) hyperphosphorylation on a circadian timescale by targeting a large number of low-affinity phosphorylation sites. Slow phosphorylation kinetics rely on site-specific recruitment of Casein Kinase 1 (CK1) and access of intrinsically disordered segments of FRQ or mPER2 to bound CK1 and on CK1 autoinhibition. Compromising CK1 activity and substrate binding affects the circadian clock in *Neurospora* and mammalian cells, respectively. We propose that CK1 and the clock proteins FRQ and PERs form functionally equivalent, phospho-based timing modules in the core of the circadian clocks of fungi and animals.**

circadian clock | CK1 | FRQ | PER | intrinsically disordered

Circadian clocks are cell-based timing systems that rhythmically optimize physiology, metabolism, and behavior according to changes associated with the 24-h day–night cycle of the earth. Despite the complexity of these processes, the core circadian clocks of fungi and animals are based on considerably simple transcriptional–translational negative feedback loops (TTFLs), in which circadian inhibitors control their own expression through rhythmic inhibition of their transcriptional activators. In constant conditions, these TTFLs oscillate in a self-sustained manner with their specific endogenous period, which is close to 24 h. The period of the oscillation is rather constant over a wide range of temperatures. The phenomenon is referred to as temperature compensation and is important for circadian timekeeping particularly in poikilotherms. Recurring extracellular cues synchronize the circadian clock through a process referred to as entrainment (1–5).

The unique ability to generate robust, self-sustained oscillations with a precise period of ∼24 h sets circadian TTFLs apart from other regulatory feedback loops in the cell. The oscillation on this time scale is made possible by the significantly delayed onset of negative feedback and its subsequent long duration. The core TTFLs of the circadian clock of *Neurospora*, *Drosophila*, and vertebrates consist of a heterodimeric transcription factor, WHITE COLLAR COMPLEX (WCC), dCLOCK/CYCLE, and CLOCK/BMAL1, respectively and a large inhibitory complex that is composed of FREQUENCY (FRQ), FRQ-Associated RNA Helicase (FRH), and Casein Kinase 1a (CK1a) in *Neurospora* (4, 5) or PERIOD (PER), TIMELESS (TIM) and the CK1 homolog DOUBLETIME (DBT) in *Drosophila* (3), or PERIOD proteins (PER1,2,3), CRYPTOCHROMEs (CRY1,2), and CK1δ/ε in vertebrates (6). Such TTFLs are interconnected with other regulatory loops that integrate and coordinate the clock with the cellular metabolism (7–13). Furthermore, interactions between clock components, their posttranslational modification, and spatiotemporal dynamics provide additional regulatory layers (2, 4–6).

Remarkably, CK1 is an essential and conserved constituent of eukaryotic circadian systems. It is a monomeric, constitutively active Ser/Thr kinase harboring an unstructured C-terminal tail (14) that can be (auto)phosphorylated (15) and inhibit the enzyme (16, 17). CK1 phosphorylates preferentially substrates that are prephosphorylated (primed) at the −3 position (18) and, with much-lower affinity, also unprimed sites (19–21). The kinase domain of CK1 contains two conserved anion (phosphate) binding sites (22, 23). Substitutions in these sites affect the substrate specificity of CK1δ (24). For example, the R178C substitution in site 1 of CK1ε, the so-called Tau mutation, reduces the kinase activity toward the primed substrates phosvitin and α-casein in vitro and results in a short-period circadian phenotype in hamster (25).

CK1 has a crucial role in the regulated turnover of FRQ and PERs. In *Neurospora*, CK1a phosphorylates FRQ (26) and is implicated in proteasomal degradation of FRQ (27, 28). In *Drosophila*, multisite phosphorylation of PER in the "per-short" domain by NEMO/NLK and DBT delays DBT-mediated phosphorylation of a distant site required for proteasomal

## Significance

Circadian clocks rely on negative feedback loops. The core circadian inhibitors, FRQ in *Neurospora* and PERs in animals, are progressively hyperphosphorylated, inactivated, and degraded. CK1 is essential for these clocks. Despite our knowledge of the role of CK1, it is not known how many other kinases are required and how multisite phosphorylation might contribute to circadian timekeeping. We show here that CK1 alone is sufficient to slowly phosphorylate low-affinity sites in FRQ or PER2. The reaction is nearly temperature compensated, and the phosphorylation state of FRQ or PER2 corresponds to the time elapsed since the start of the reaction. Thus, CK1 and FRQ or PER2 form equivalent modules that are in principle capable of measuring time on a circadian scale.

BIOCHEMISTRY

degradation of PER (29, 30). A similar phosphoswitch modulates the circadian clock of vertebrates (31): the S662G substitution in human PER2 causes familial advanced sleep phase syndrome (FASPS) (32) and prevents priming (33) and subsequently priming-dependent phosphorylation by CK1δ/ε of an array of sites (34–36). Phosphorylation of the FASPS site attenuates the phosphorylation of a distant degron recognized by the E3-ligase β-TrCP (31), which triggers proteasomal degradation of PER2 (31–39). In addition, CK1-dependent hyperphosphorylation of FRQ and PERs also favors conformations that compromise their function and concomitantly promotes the turnover of these clock proteins (28, 34, 40, 41).

Thus, mounting evidence indicates that time measurement at the molecular level is intertwined with hyperphosphorylation of FRQ and PERs. However, while it is fairly well understood that phosphorylation modulates circadian period length, how multisite phosphorylation of clock proteins could be related to the measurement of a 24-h time period is unknown.

Here, we show that CK1 is sufficient to support in vitro the steadily progressing phosphorylation of FRQ and mPER2 at low-affinity sites on a timescale suitable to measure the length of a day. Site-specific recruitment of CK1 to FRQ and PERs and autoinhibition of the kinase are key to achieve such slow phosphorylation kinetics. Manipulations that increase CK1 levels or activity shorten the circadian period in *Neurospora* and in human cell lines. We thus propose that the CK1a–FRQ and the CK1δ–PER2 complexes represent functionally equivalent timing modules suitable to act as core pacemakers of circadian clocks in fungi and mammals.

## Results

### Characterization of the Priming-Dependent and -Independent Activity of CK1.
CK1 is an essential kinase in the circadian clocks of fungi and animals. To characterize the activity of *Neurospora* CK1a toward primed and unprimed substrate, we produced N-terminally His-tagged *Neurospora* CK1a, the Tau-like CK1a mutant, CK1a-R181Q, and the CK1aΔC version lacking the C-terminal tail (*SI Appendix*, Fig. S1A). We produced the R-to-Q rather than the original R-to-C substitution to assess whether the Tau phenotype is independent of potential redox-related properties of the sulfhydryl group. CK1a and CK1a-R181Q were autophosphorylated to the same extent, while CK1aΔC was not (*SI Appendix*, Fig. S1B). Nano differential scanning fluorimetry (nano DSF) analysis showed thermal unfolding of the three recombinant *Neurospora* kinases at about 45 °C (*SI Appendix*, Fig. S1C), indicating that the proteins were folded in the same manner.

We then measured the phosphorylation kinetics at 20 °C of a peptide that was prephosphorylated at the −3 position and sulfonamido-oxine (SOX) labeled at its C terminus (pSxxS: KRRRALSpS-VASL-SOX) such that it exhibited $Mg^{2+}$ chelation–enhanced fluorescence (ChEF) upon phosphorylation at the +1 position. CK1a-R181Q was about 11-fold less active than CK1a (Fig. 1A and Table 1), in line with the Tau mutation in mammalian CK1ε compromising recognition of primed substrates (25). CK1aΔC was about 1.4-fold more active than CK1a (Fig. 1A and Table 1), indicating that CK1a was slightly inhibited by its autophosphorylated C-terminal tail.

To characterize the priming-independent activity of the kinases, we used the same peptide upon an S-to-A substitution in the −3 position (AxxS: KRRRALSAVASL-SOX). CK1a and CK1aΔC phosphorylated the unprimed AxxS peptide 182-fold and 113-fold, respectively, slower than the primed peptide (Fig. 1B and Table 1). CK1a-R181Q phosphorylated the AxxS peptide only about 18-fold slower than the primed peptide and thus with similar kinetics as CK1a (Fig. 1B). The data indicate that CK1a, like other CK1 family members, preferentially
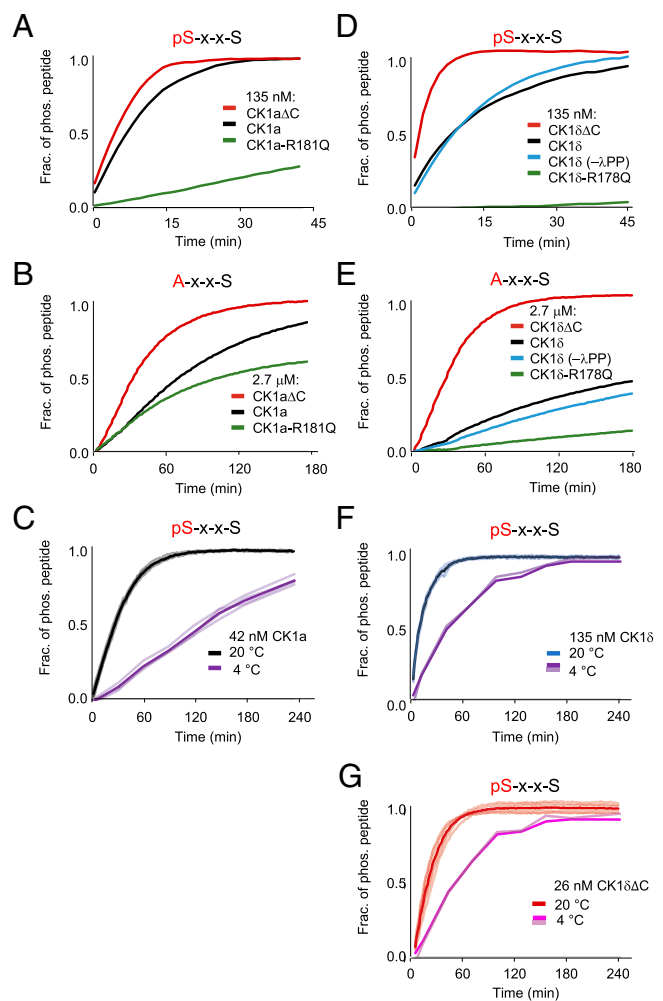


**Fig. 1.** Activity of CK1a and CK1δ variants. (A) Priming-dependent activity of CK1a variants. ChEF assay with 135 nM of the indicated recombinant CK1a version and 10 μM primed SOX-labeled peptide (pS-x-x-S). The curve represents the average of six measurements. (B) CK1a displays low affinity for unprimed peptide. A ChEF assay was carried out with 10 μM unprimed SOX-labeled peptide (A-x-x-S) and 2.7 μM (20-fold higher than in A) of the indicated recombinant CK1a version. (C) Temperature-dependent activity of CK1a. ChEF assay was carried out at 20 °C as described in A but with 42 nM recombinant CK1a. Solid curve represents the average of six measurements (gray curves). Phosphorylation of pS-x-x-S at 4 °C was measured at t = 0, 30, 60, 90, 120, 180, and 240 min as described in experimental procedures (further time points are shown in Dataset S6). Solid purple curve represents the average of four replicates (light purple curves). (D) Priming-dependent activity of CK1δ variants. ChEF assay was carried as in A. CK1δ and CK1δ-R178Q were unphosphorylated, and CK1δ (-λPPase) was autophosphorylated. (E) Priming-independent activity of CK1δ variants. ChEF assay was carried out as in B. (F and G) Temperature-dependent activity of CK1δ (F) and CK1δΔC (G). ChEF assay was carried out at 20 °C as described in A. The solid red curve represents the average of six measurements (light red curves). Phosphorylation of pS-x-x-S at 4 °C was measured at t = 0, 10, 40, 70, 100, 130, 160, 190, and 250 min as described in experimental procedures (further time points are shown in Dataset S6). The number of replicates is indicated.

catalyzes phosphate-directed phosphorylation. The Tau-like substitution, R181Q, affects predominantly priming-dependent activity and, to a much-lesser extent, priming-independent activity of CK1a.

To assess the temperature dependence of the kinase reaction, we measured the activity of CK1a at 4 and 20 °C (Fig. 1C). The phosphorylation kinetics of the pSxxS peptide were 4.8-fold slower at 4 than at 20 °C (Table 1), demonstrating that

**Table 1. Activity of CK1 variants**

A

|  | Primed peptide (Phosphorylation per min) | ± SEM | Unprimed peptide (Phosphorylation per min) | ± SEM | Ratio primed/ unprimed |
|---|---|---|---|---|---|
| CK1aΔC | 6.063 | 0.400 | 0.054 | 0.004 | 113 |
| CK1a | 4.441 | 0.190 | 0.024 | 0.001 | 182 |
| CK1a-R181Q | 0.405 | 0.017 | 0.023 | 0.001 | 18 |
| CK1δΔC | 12.138 | 0.966 | 0.061 | 0.001 | 198 |
| CK1δ | 4.078 | 0.275 | 0.012 | 0.000 | 328 |
| CK1δ (–λPP) | 3.996 | 0.189 | 0.009 | 0.000 | 468 |
| CK1δ-R178Q | 0.078 | 0.007 | 0.002 | 0.000 | 35 |

B

|  | Primed peptide (Phosphorylation per min) at 20 °C | ± SEM | Primed peptide (Phosphorylation per min) at 4 °C | ± SEM | Ratio 20 °C/4 °C |
|---|---|---|---|---|---|
| CK1a | 4.495 | 0.119 | 0.940 | 0.047 | 4.781 |
| CK1δ | 4.078 | 0.275 | 0.770 | 0.019 | 5.295 |
| CK1δΔC | 12.138 | 0.966 | 4.344 | 0.065 | 2.795 |

A: Priming-dependent and independent kinase activity and B: temperature-dependent kinase activity of CK1a and CK1δ. Reaction rates were determined from the initial slopes of peptide phosphorylation kinetics shown in Fig. 1.

the catalytic activity of CK1a was temperature dependent with a $Q_{10}$ of ~2.7 ($Q_{10} = 4.8^{10/(20 - 4)}$).

We then set out to analyze the kinase activity of human CK1δ toward the primed and unprimed peptides. Therefore, we produced His- and FLAG-tagged human CK1δ and the constitutively active version, CK1δΔC, which was truncated after residue F295 and hence lacks its autoinhibitory C-terminal tail (15, 42) (*SI Appendix*, Fig. S1D). When expressed in *Escherichia coli*, CK1δ was autophosphorylated at its tail, while coexpression of λ-phosphatase antagonized autophosphorylation of CK1δ (*SI Appendix*, Fig. S1E). In addition, we coexpressed λ-phosphatase and the Tau-like version CK1δ-R178Q. Nano DSF analysis of the purified proteins showed unfolding of all CK1δ versions at about 55 °C (*SI Appendix*, Fig. S1F), indicating that the proteins were stably folded. The 10 °C higher thermal stability of CK1δ in comparison to CK1a may reflect adaptation to the different optimal growth temperatures of mammals and fungi.

When unphosphorylated CK1δ and CK1δ-R178Q were incubated with ATP, they autophosphorylated in a temperature-dependent fashion (*SI Appendix*, Fig. S1G), similar to what has been previously reported (43).

We then measured at 20 °C the phosphorylation kinetics of the primed peptide, pSxxS. To our surprise, autophosphorylated and dephosphorylated CK1δ phosphorylated pSxxS with similar kinetics, even in the initial phase of the reaction (Fig. 1D) when the dephosphorylated CK1δ had not yet autophosphorylated to a substantial extent. CK1δΔC phosphorylated pSxxS about threefold faster than unphosphorylated or autophosphorylated CK1δ (Fig. 1D and Table 1). The data indicate that the C-terminal tail attenuated phosphorylation of pSxxS. However, the autoinhibition was only slightly affected by autophosphorylation. CK1δ-R178Q was about 52-fold less active than CK1δ (see Fig. 4B and Table 1), showing that this Tau-like version had a severely compromised priming-dependent kinase activity.

We then measured the phosphorylation kinetics of the unprimed peptide, AxxS (Fig. 1E). Unphosphorylated and autophosphorylated CK1δ phosphorylated the AxxS peptide 328-fold and 468-fold slower, respectively, than the pSxxS peptide (Table 1). However, since autophosphorylation of the initially unphosphorylated CK1δ (*SI Appendix*, Fig. S1G) was faster than phosphorylation of AxxS, it was not possible to assess the impact of autophosphorylation on the kinase activity

toward unprimed peptide. The constitutively active CK1δΔC phosphorylated the AxxS peptide 2.3-fold faster than CK1δ (Fig. 1E and Table 1).

CK1δ-R178Q was about sixfold less active than CK1δ toward AxxS (Fig. 1E), as compared to its 52-fold lower activity than CK1δ toward pSxxS (Fig. 1D). Thus, the Tau-like substitutions in CK1a and CK1δ attenuated predominantly phosphorylation of primed peptide (Table 1), consistent with a role of the positively charged Tau site in accommodating the phosphate of primed substrate (25) and to a lesser extent phosphorylation of unprimed peptide (Table 1), presumably because the substitution affected the conformation of the activation loop of the kinases (24).

Phosphorylation of a primed peptide by CK1δΔC was recently reported to be rather well temperature compensated ($Q_{10} = 1.42$) between 25 and 35 °C (44). We measured the activity of CK1δ and CK1δΔC at 4 and 20 °C (Fig. 1 F and G). CK1δ and CK1δΔC phosphorylated pSxxS ca. 5.3-fold and 2.8-fold, respectively, slower at 4 than at 20 °C (Table 1). Hence, the kinase activity was temperature dependent over this range with a $Q_{10}$ of ~2.8 ($Q_{10} = 5.3^{10/(20 - 4)}$) and 1.9, respectively. The data suggest that the C-terminal tail affects the temperature dependence of the CK1δ activity.

**CK1a Recruitment Drives Priming-Independent Hyperphosphorylation of FRQ.** More than 100 phosphorylation sites contribute to the hyperphosphorylated state of FRQ in vivo (45, 46). However, only 19 of these sites match the consensus for potential priming-dependent phosphorylation by CK1a (*SI Appendix*, Fig. S2A), implying that FRQ is phosphorylated by CK1a mainly in a priming-independent manner and/or by other kinases. Indeed, 43 FRQ sites were found to be phosphorylated by CK1a in vitro, and only five of them were potentially phosphorylated in a (self) priming-dependent fashion (46). Thus, we analyzed priming-independent phosphorylation of FRQ by CK1a. To this end, we incubated recombinant wild-type CK1a or its R181Q mutant with purified recombinant short FRQ (sFRQ), a functional splice isoform of FRQ (47). Reactions were carried out under pseudo first-order conditions (CK1a, CK1a-R181Q ≫ sFRQ) at 4 and 20 °C. Surprisingly, CK1a and CK1a-R181Q both progressively phosphorylated sFRQ over a time course of 24 h and longer with similar kinetics (Fig. 2 A, *Upper*, Fig. 2B, and *SI Appendix*, Fig. S2B). The kinetics were
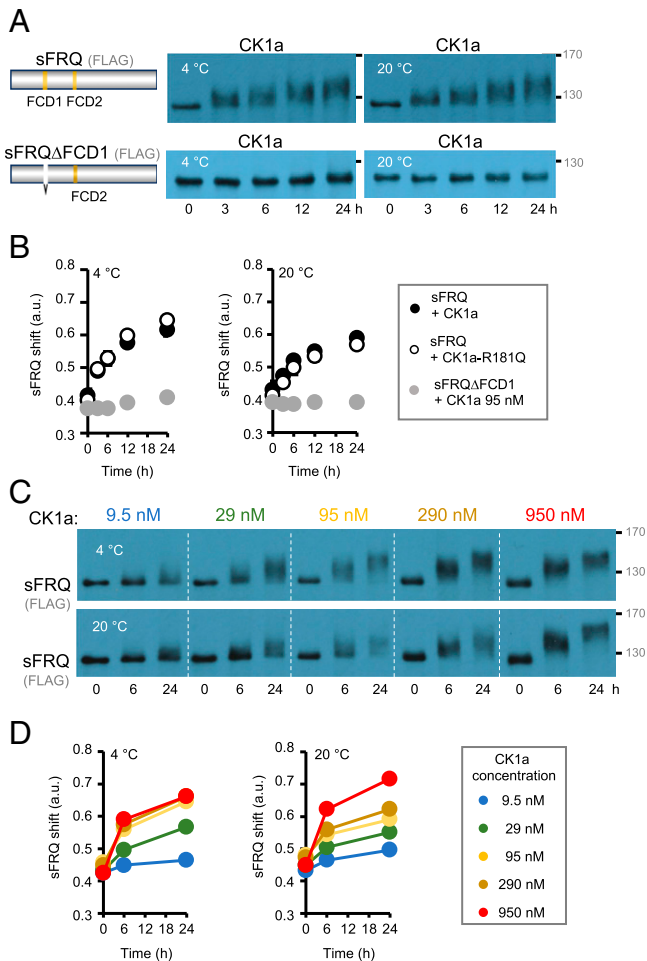
**Fig. 2.** CK1a supports progressive hyperphosphorylation of sFRQ in vitro. (*A*) Hyperphosphorylation kinetics of sFRQ are independent of priming but requires CK1a recruitment. (*Upper*) sFRQ (8.3 nM) was incubated with CK1a (95 nM) and an ATP regenerating system at 4 and 20 °C for up to 24 h. (*Lower*) CK1a does not hyperphosphorylate sFRQΔFCD1. Phosphorylation kinetics were analyzed by Western blot with FLAG antibodies. Molecular mass standards are indicated. (*B*) Quantification of phosphorylation kinetics such as shown in *A*. The electrophoretic position of the center of mass of sFRQ was determined by densitometry, and the electrophoretic shift (sFRQ shift) was blotted relative to molecular mass standards. The electrophoretic positions of the 95- and 170-kDa molecular mass markers were set arbitrarily to 0 and 1, respectively. Error bars indicate ± SEM, n = 3 for CK1a and range, and n = 2 for CK1a-R181Q, except n = 1 for 3 h time points and n = 1 for sFRQΔFCD1. (*C*) Phosphorylation kinetics of sFRQ are dependent on CK1a concentration and slightly more efficient at 4 than at 20 °C. FRQ (8.3 nM) was incubated with the indicated concentrations of CK1a for the indicated time periods (n = 1). (*D*) Quantification of phosphorylation kinetics shown in *C*.

slightly faster at 4 than at 20 °C. The data show that CK1a can hyperphosphorylate FRQ in a priming-independent manner and rather independent of temperature, in contrast to its temperature-dependent activity toward peptide (Fig. 1*C*). However, CK1a did not hyperphosphorylate sFRQΔFCD1, a FRQ version which cannot recruit the kinase (28), indicating that priming-independent phosphorylation requires binding of CK1a to FRQ (Fig. 2 *A*, *Lower*, and *B*).

To characterize the CK1a–FRQ equilibrium, sFRQ was phosphorylated at 4 and 20 °C with different concentrations of CK1a. The phosphorylation kinetics of sFRQ increased with increasing CK1a concentrations approaching maximal kinetics at about 95 nM CK1a at 4 °C and at 950 nM CK1a at 20 °C,

indicating that the CK1a activity had reached functional saturation (Fig. 2 *C* and *D*).

In contrast, phosphorylation of sFRQΔFCD1 was severely impaired under such conditions, and only at 950 nM did CK1a phosphorylate sFRQΔFCD1 to a detectable extent (*SI Appendix*, Fig. S2*C*).

We then phosphorylated sFRQ with CK1aΔC. The C-terminally truncated kinase phosphorylated sFRQ faster than CK1a and reached saturation at lower kinase concentration (*SI Appendix*, Fig. S2 *D* and *E*), consistent with its higher activity.

Together, these data demonstrate that CK1a alone can hyperphosphorylate recombinant FRQ in a steadily progressing and rather temperature-independent manner over a long time period (>24 h). Hence, CK1a and FRQ are in principle suited to measure time on a circadian scale. This reaction is independent of priming but requires FCD-dependent recruitment of CK1a to FRQ, which facilitates the phosphorylation of low-affinity sites in FRQ. The phosphorylation kinetics are slowed by the autophosphorylated C-terminal tail of CK1a.

**CK1a Phosphorylates a Subset of Sites in sFRQ in a Priming-Dependent Fashion.** We next set out to characterize priming-dependent phosphorylation of FRQ by CK1a. In order to detect priming-dependent phosphorylation, we suppressed priming-independent phosphorylation of low-affinity sites by exploiting sFRQΔFCD1 as a substrate, since CK1a alone did not phosphorylate this protein (Fig. 2*A*). We reasoned that phosphorylation of high-affinity primed sites by CK1a (100-fold higher affinity than unprimed sites) did not require recruitment of CK1a to sFRQ. As priming kinases of CK1a are not known, we used native whole-cell lysate prepared from *Saccharomyces cerevisiae* (yWCL) as a fairly general source of potential priming kinases. It should be noted that Hrr25, the yeast homolog of CK1a, does not support hyperphosphorylation of FRQ (48). Upon incubation with yWCL for up to 24 h, a very small fraction of sFRQΔFCD1 was converted to a rather-distinct phosphospecies (Fig. 3 *A*, *Upper*), indicating that the yeast kinases present in the yWCL cannot efficiently drive sFRQΔFCD1 hyperphosphorylation. Addition of the priming-deficient CK1a-R181Q did not enhance phosphorylation of sFRQΔFCD1 in the presence of yWCL (Fig. 3 *A*, *Lower*). However, addition of CK1a together with yWCL efficiently converted sFRQΔFCD1 into a distinct phosphospecies (Fig. 3*B*). The phosphorylation kinetics were faster at 20 than at 4 °C, in good agreement with the purported involvement of temperature-dependent priming kinases. This strongly suggests that yWCL phospho-primed sFRQΔFCD1, the phosphorylation of which was taken over by CK1a but not by CK1a-R181Q. Priming-dependent phosphorylation was fast and did not require FCD-dependent recruitment of CK1a to FRQ, consistent with the higher affinity of CK1a for primed substrate (Table 1).

The specific priming-dependent phosphospecies of sFRQΔFCD1 were clearly distinct from the heterogeneously hyperphosphorylated sFRQ species generated in a priming-independent reaction. To allow priming-dependent as well as priming-independent phosphorylation we incubated sFRQ with CK1a and yWCL (Fig. 3*C*). At 4 °C, when priming-dependent phosphorylation was rather slow, sFRQ was predominantly phosphorylated in a priming-independent manner, while at 20 °C, priming-dependent phosphorylation species prevailed (Fig. 3 *C* and *D*). Under these conditions, priming-independent hyperphosphorylation of sFRQ was delayed (arrows).

In summary, CK1a in cooperation with general cellular kinase(s) can phosphorylate sFRQ with high affinity at a subset of sites, and priming-dependent phosphorylation slows priming-independent hyperphosphorylation of sFRQ. Hence, priming-dependent phosphorylation of FRQ is expected to lengthen period similar to the priming-dependent phosphorylation of *Drosophila* PER (40) and mammalian PER2 (31).
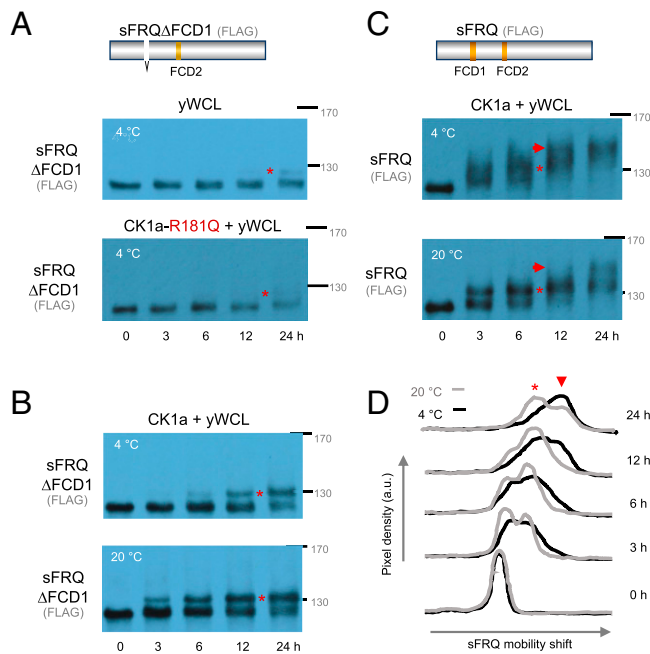
**Fig. 3.** Priming-dependent phosphorylation of sFRQ by CK1a. (*A*) Kinases present in yWCL and CK1a-R181Q, deficient in priming-dependent phosphorylation, do not support efficient phosphorylation of sFRQΔFCD1. sFRQΔFCD1 (8.3 nM) was incubated with 200 μg yWCL with and without CK1a-R181Q (95 nM) for the indicated time periods. The asterisk indicates the position of phosphospecies generated with low efficiency. (*B*) CK1a supports priming-dependent phosphorylation in an FCD1-independent manner. YWCL (200 μg) was incubated with CK1a (95 nM) and FRQΔFCD1 (8.3 nM) at 4 and 20 °C. The generated phosphospecies is indicated by the asterisk. (*C*) Priming-dependent phosphorylation delays priming-independent phosphorylation of sFRQ. Phosphorylation kinetics of sFRQ (8.3 nM) by CK1a (95 nM) in the presence of yWCL at 4 °C are similar to the priming-independent phosphorylation in absence of WCL (Fig. 3*A*). At 20 °C, phosphospecies dependent on yWCL and CK1 are rapidly generated (asterisk) and priming-independent progressive phosphorylation is delayed (arrow). (*D*) Densitometric traces show the electrophoretic mobility shift of sFRQ (shown in *C*) upon phosphorylation by CK1a at 4 °C (black traces) and 20 °C (gray traces). The asterisk indicates the position of the priming-dependent phosphospecies, and the arrow indicates the delayed generation of highly phosphorylated sFRQ at 20 °C.

## Recruitment of CK1δ Drives Priming-Independent Phosphorylation of mPER2.

Mammalian PERs are progressively hyperphosphorylated in the course of a circadian day. CK1δ/ε are crucial for circadian rhythmicity, but it is not known to what extent CK1δ/ε contributes to the phosphorylated state of PERs. Therefore, we studied how wild-type and mutant CK1δs affect the phosphorylation of mPER2 in a cell-free system. Upon transient transfection of HEK293 cells, overexpressed V5-tagged mPER2 accumulated in a hyperphosphorylated form, suggesting that endogenous kinases were limiting.

Native WCLs from these cells were incubated at 4 °C with recombinant unphosphorylated and autophosphorylated CK1δ, respectively, in excess over mPER2. CK1δ progressively hyperphosphorylated mPER2 over a time course of 24 h (Fig. 4 *A, Left*), indicating that CK1δ is sufficient to slowly phosphorylate mPER2 on a circadian time scale.

In contrast, autophosphorylated CK1δ did not support hyperphosphorylation of mPER2 (Fig. 4 *A, Right*). Considering that autophosphorylation of CK1 did not significantly affect the phosphorylation of primed peptide (pSxxS), the phosphorylation state of the C-terminal tail seems to particularly affect the hyperphosphorylation of mPER2. To estimate the effects of autophosphorylation, we preincubated unphosphorylated CK1δ

with ATP for various time periods to allow autophosphorylation of the kinase and then added mPER2 for a fixed period of 6 h to determine residual CK1δ activity. The activity of CK1δ decreased gradually with increasing preincubation time (*SI Appendix*, Fig. S3*A*). Comparison with the autophosphorylation kinetics of CK1δ (*SI Appendix*, Fig. S1*G*) suggests that only highly autophosphorylated CK1δ species were efficiently inhibited in their activity toward mPER2.

Next, we phosphorylated mPER2 with unphosphorylated CK1δ and CK1δ-R178Q at 4 and 20 °C. Surprisingly, CK1δ and CK1δ-R178Q phosphorylated mPER2 with similar kinetics (Fig. 4*B*). Considering that primed peptide was phosphorylated ~50-fold faster by CK1δ than by CK1δ-R178Q, the data suggest that the majority of mPER2 phosphorylation was not dependent on self-priming. The phosphorylation kinetics of mPER2 were dependent on the concentration of CK1δ but was rather similar at 4 and 20 °C (Fig. 4 *A* and *C*), suggesting that the reaction was almost temperature compensated.

The constitutively active enzyme CK1δΔC phosphorylated mPER2 faster than CK1δ or CK1δ-R178Q (*SI Appendix*, Fig. S3*B*), suggesting that the kinases autophosphorylated and increasingly inhibited themselves as the in vitro reactions proceeded.

Together, the data indicate that the PER2 phosphorylation kinetics by CK1δ were temperature compensated and not limited by the temperature-dependent enzymatic activity of the kinase. We therefore asked whether hyperphosphorylation of mPER2 depends on CK1δ recruitment. An mPER2 mutant (mPER2ΔCKBD) lacking the CK1δ-binding site, located between residues 554 and 763 (32) (Fig. 4*D*), was thus expressed in HEK293 cells, and we then analyzed phosphorylation of this mutant protein. Phosphorylation of mPER2ΔCKBD was impaired at 42 nM but not at 840 nM CK1δ (Fig. 4*D* and *SI Appendix*, Fig. S3*C*), suggesting that substrate-binding was limiting for mPER2 hyperphosphorylation at low CK1δ concentrations but dispensable at high concentrations. The data demonstrate that recruitment of CK1δ increases the local kinase concentration to drive phosphorylation of low-affinity sites in mPER2. A detailed functional analysis of the CKBD (37) demonstrated previously that the deletion of residues 582 through 606 or 731 through 756 of mPER2 compromises the recruitment of CK1ε. We found that these regions, which were recently termed CK1BD-A and CK1BD-B (49), have the potential to form amphipathic α-helices (Fig. 4 *E, Left*) similar to FCD1 and FCD2 of *Neurospora* FRQ (28). Next, we expressed mPER2ΔCK1BD-A and mPER2ΔCK1BD-B in HEK293 cells and found that their phosphorylation at low CK1δ concentration was decreased (Fig. 4 *E, Right*).

Taken together, our data suggest that efficient hyperphosphorylation of mPER2 is supported by recruitment of CK1δ to CKBD (casein kinase binding domain), assisted by CK1BD-A and CK1BD-B, to increase local kinase concentration, thereby enabling priming-independent progressive phosphorylation of low-affinity sites.

## CK1δ Expression and Its Priming-Independent Phosphorylation Activity Determine Circadian Period Length in Mammalian Cells.

To assess how CK1δ impacts the circadian clock in living cells, we generated stable T-Rex-U2OS cells expressing in a doxycycline (DOX)-inducible manner either CK1δ, or CK1δ-R178Q, or the catalytically inactive CK1δ-K38R mutant (50).

T-REx-U2OS cells expressing the CK1δ versions were then grown with or without DOX. Transiently transfected p*Bmal1-luc* reporter plasmid (51) allowed us to monitor the circadian period for 96 h (Fig. 5*A*). CK1δ overexpression shortened the circadian period by about 2 h relative to the uninduced cells (phosphate buffered saline [PBS]). Hence, endogenous CK1 activity was functionally not saturating in T-REx-U2OS cells. More importantly, CK1δ-R178Q expression shortened the
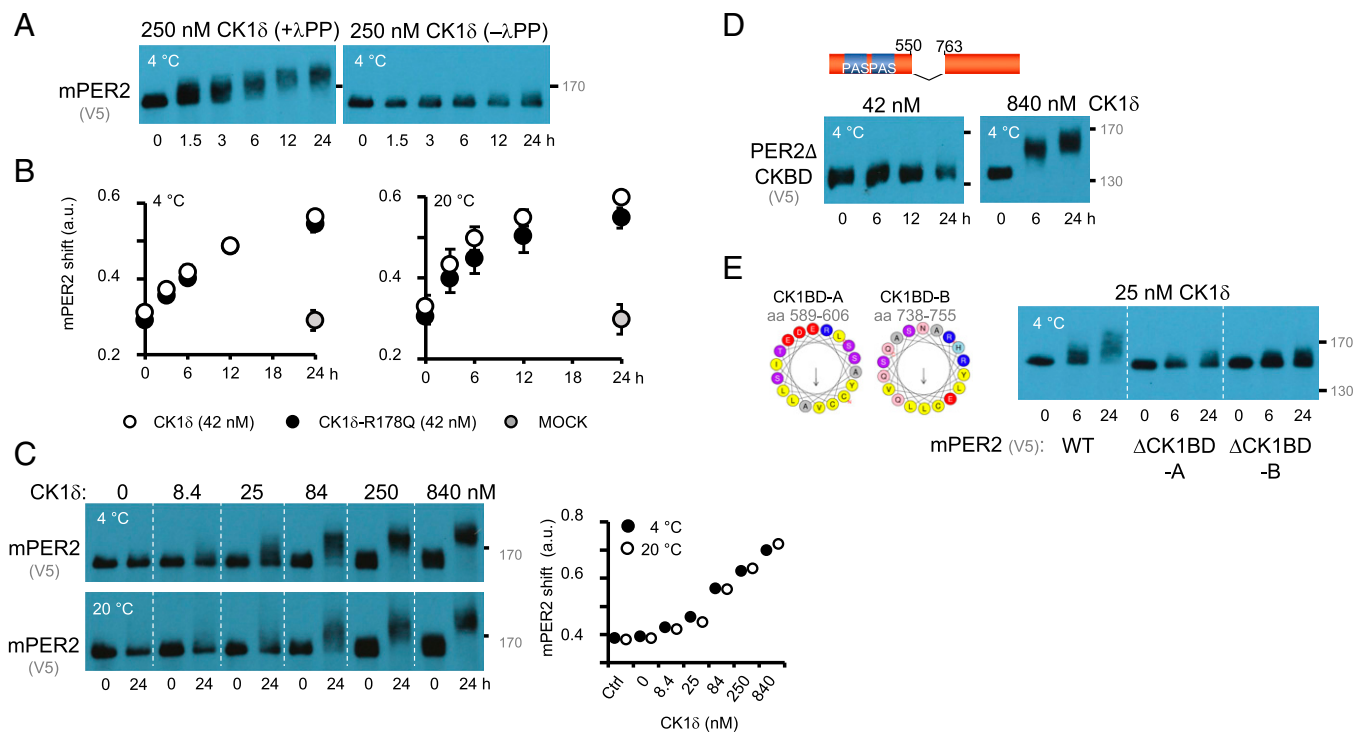
Marzoll et al.
Casein kinase 1 and disordered clock proteins form functionally equivalent, phospho-based circadian modules in fungi and mammals

PNAS | 5 of 10
https://doi.org/10.1073/pnas.2118286119

**Fig. 4.** Hyperphosphorylation of mPER2 by CK1δ in vitro is facilitated by substrate-binding and does not require priming. (*A*) Hyperphosphorylation of mPER2 in vitro is strongly inhibited by autophosphorylation of CK1δ. In total, 250 nM unphosphorylated CK1δ (+λPP) and autophosphorylated CK1δ (−λPP), respectively, were incubated with V5-tagged mPER2 (mPER2) transiently expressed in HEK293 cells (*SI Appendix, SI Methods*). The phosphorylation kinetics of mPER2 by CK1δ were analyzed by Western blot. (*B*) CK1δ and the Tau-like version CK1δ-R178Q hyperphosphorylate mPER2 with similar kinetics and in a temperature-independent fashion. Quantification of mPER2 phosphorylation kinetics by CK1δ and CK1δ-R178Q at 4 (*Left*) and 20 °C (*Right*) is shown. mPER2 was incubated with 42 nM CK1δ (open circles) or CK1δ-R178Q (black circles) for the indicated time periods and then analyzed by Western blot as shown in *A*. The electrophoretic position of the center of mass of mPER2 was determined by densitometry and blotted relative to the molecular mass standards. The electrophoretic positions of the 130- and 170-kDa molecular mass markers were set arbitrarily to 0 and 0.5, respectively (gray circle: 24-h mock incubation without added kinase). Error bars are ± SEM, n = 3 for CK1δ, and n = 2 for CK1δ-R178Q and mock. (*C*) Phosphorylation of mPER2 is dependent on CK1δ concentration at 4 and at 20 °C. Quantification was performed as in *B* (n = 1). Ctrl = no kinase added, 0 min incubation. (*D*) Hyperphosphorylation of mPER2 by CK1δ is facilitated by CKBD. (*Top*) Schematic of PER2ΔCKBD, lacking the CK1-binding domain, aa 554 through 763 (32). (*Bottom*) mPER2ΔCKBD is not hyperphosphorylated by 42 nM CK1δ but efficiently hyperphosphorylated by 840 nM CK1δ. (*E*) CK1BD-A and CK1BD-B facilitate hyperphosphorylation of mPER2 by CK1δ. (*Left*) PER2–CK1 interaction domain A (CK1BD-A) and CK1BD-B(37, 49) have the potential to form amphipathic helices (https://heliquest.ipmc.cnrs.fr) (67). (*Right*) Phosphorylation kinetics of mPER2, mPER2ΔCK1BD-A, and mPER2ΔCK1BD-B by 25 nM CK1δ.

circadian period even more markedly (ca. 7 h) (Fig. 5 *A* and *B*). In contrast, the catalytically inactive CK1δ-K38R lengthened and severely attenuated the circadian rhythm (Fig. 5 *A* and *B*), suggesting a dominant negative effect, presumably by occupying PER's CKBD. Similarly, period-lengthening was observed in *Drosophila* when DBT was replaced by a catalytically inactive K38R variant (52). An additional wild-type copy of DBT did not shorten period length, presumably because DBT was not appreciably overexpressed (52).

Together, the data indicate that the expression level of CK1δ can affect the circadian period length through activity that does not require priming in addition to the well-established impact of the priming-dependent activity of the kinase on period.

**CK1a and CK1δ Have Conserved Circadian Clock Regulatory Functions.** The catalytic domains of mammalian CK1δ and *Neurospora* CK1a are highly conserved (*SI Appendix*, Fig. S4*A*), suggesting that they might regulate the circadian clock in a similar way. We thus incubated mPER2 with CK1a or CK1a-R181Q at 4 and 20 °C and found that both kinases hyperphosphorylated mPER2 with identical kinetics and in an almost temperature-compensated fashion (*SI Appendix*, Fig. S4*B*). The data demonstrate that *Neurospora* CK1a, just like CK1δ, can hyperphosphorylate mPER2 in a priming-independent fashion. CK1a and CK1a-R181Q phosphorylated PER2 slower than the

cognate human versions (*SI Appendix*, Fig. S4*B* and Fig. 4*B*). CK1aΔC rapidly and efficiently phosphorylated mPER2 (*SI Appendix*, Fig. S4*C*), indicating that hyperphosphorylation of mPER2 by full-length CK1a was attenuated by autoinhibition of the kinase by its C-terminal tail. CK1a did not hyperphosphorylate mPER2ΔCKBD to a substantial extent (*SI Appendix*, Fig. S4*D*), suggesting that the reaction was dependent on the recruitment of CK1a to the CKBD of PER2.

Next, we expressed CK1a and CK1a-R181Q in T-REx-U2OS cells. Induction of the *Neurospora* kinases shortened the circadian period to the same extent as their cognate human versions (Fig. 5*B* and *SI Appendix*, Fig. S4*E*). Therefore, *Neurospora* CK1a, just like human CK1δ, can impact the mammalian circadian clock through its priming-independent phosphorylation activity.

Finally, overexpression of CK1a in *Neurospora* shortened circadian period length (Fig. 5*C*). Together, the data indicate that CK1 expression levels are not saturating and determine circadian period length in *Neurospora* and in U2OS cells.

## Discussion

The essential role of CK1 in circadian clocks has been documented beyond doubt in several systems. Yet, it is not known how circadian clocks measure time on the molecular level and how CK1 contributes to this process. We show here that CK1a and
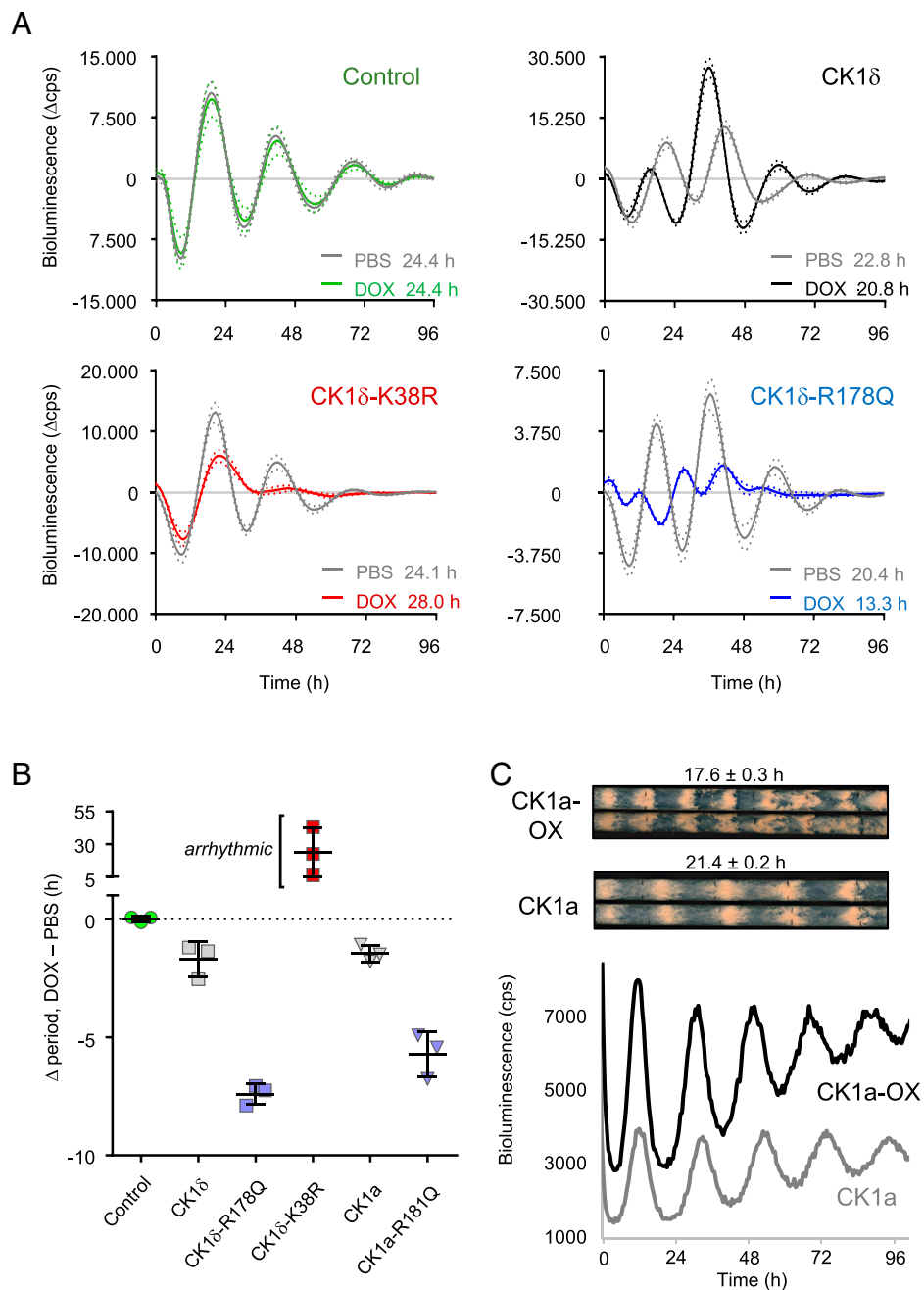
**Fig. 5.** CK1δ variants affect the circadian period in T-REx-U2OS cells. (*A*) Luciferase reporter assay. T-REx-U2OS control cells (*Upper Left*) and T-REx-U2OS cells expressing the indicated CK1δ versions in a DOX-inducible manner were transiently transfected with a p*Bmal1-luc* reporter plasmid (51). Bioluminescence data were detrended. Dotted lines represent SD (± SD) of four technical replicates. Circadian period length in presence and absence of DOX is indicated (note that the period length of CK1δ and CK1δ-R178Q cells in absence of DOX is already shortened compared to control cells). (*B*) Expression of CK1δ versions affects circadian period length. Each symbol represents an independent biological replicate with four technical replicates as shown in *A*. Data are presented as mean ± SD. (*C*) Overexpression of CK1a in *Neurospora* shortens circadian period length. (*Upper*) CK1a was overexpressed in *Neurospora*, and the circadian conidiation rhythm was analyzed by race-tube assay. (*Lower*) CK1a was overexpressed in a *Neurospora* strain harboring a *frq-lucPEST* reporter gene (68). A 96-well plate with luciferin medium was inoculated with conidia, and bioluminescence was recorded at 25 °C in darkness as described (69). Traces are averages of at least eight replicates.

CK1δ by themselves are capable of slowly and robustly hyper-phosphorylating FRQ and mPER2 in a priming-independent manner in vitro. The phosphorylation kinetics of FRQ and mPER2 were almost temperature compensated and progressed steadily for more than 24 h over a broad range of kinase concentrations. Since these proteins are expressed and interact in vivo, they have the potential to perform corresponding reactions in living fungi and animals. We therefore hypothesize that the evolutionarily conserved CK1, together with the nonorthologous clock proteins FRQ and PERs, respectively, might represent functionally equivalent core clock modules that measure circadian time through steadily progressing and often functionally redundant priming-independent hyperphosphorylation. Priming-dependent phosphorylation by CK1 of specific sites in these clock proteins and phosphorylation of clock proteins by other kinases could crucially modulate the circadian clock (e.g., in response to
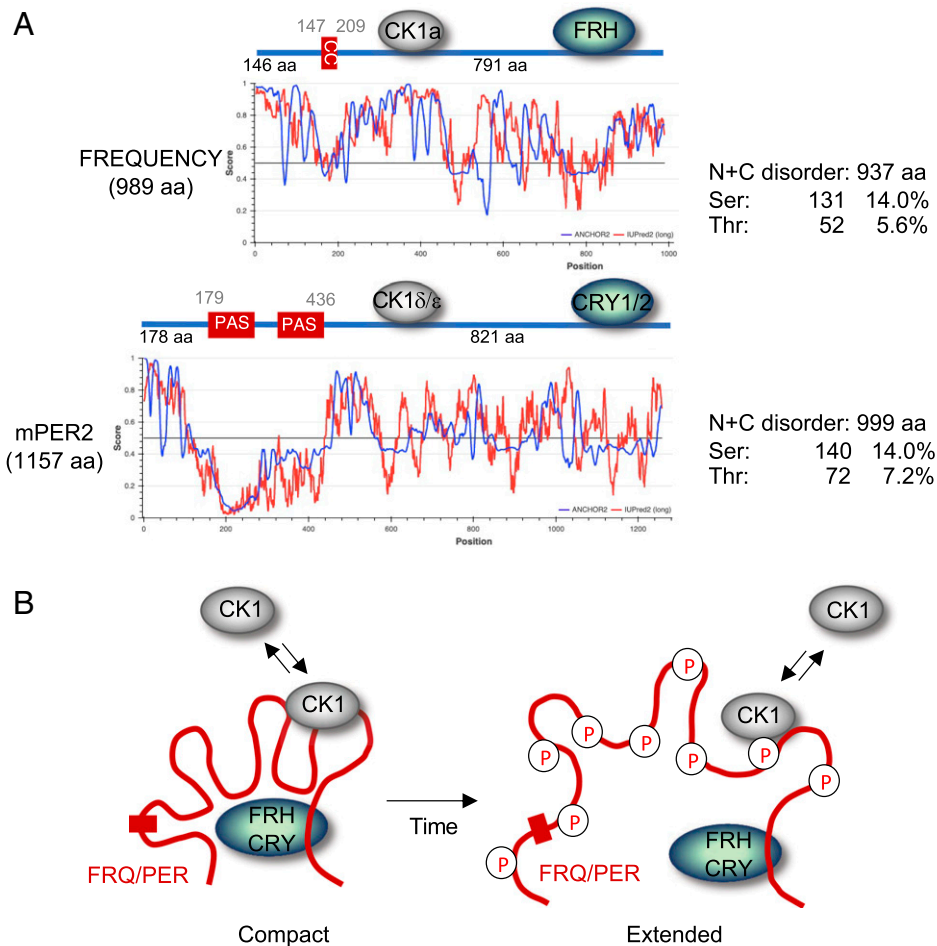
Marzoll et al.
Casein kinase 1 and disordered clock proteins form functionally equivalent, phospho-based circadian modules in fungi and mammals

PNAS | 7 of 10
https://doi.org/10.1073/pnas.2118286119

**Fig. 6.** CK1 forms equivalent complexes with FRQ and mPER2. (*A*) FRQ and mPER2 share a similar architecture and IDRs of similar size. Schematic and disorder plot of FRQ (*Upper*) and mPER2 (*Lower*). Dimerization domains are indicated by red boxes: coiled-coil domain (CC) in FRQ (A147 through A209) and PAS-PAS domains in mPER2 (I179 through P436). Binding of CK1a and CK1δ/ε to the central portions and of FRH and CRYPTOCHROMEs (CRY1/2) to the C-terminal portions of FRQ and mPER2, respectively, is shown. Plots were generated by IUPred2A-long (red) and ANCHOR2 (blue). The total lengths of the regions N- and C-terminal of the dimerization domains and their seryl and threonyl content are indicated. They are largely predicted to be disordered and hence referred to as N + C disorder. (*B*) Model of functionally equivalent circadian phospho-timers in fungi and mammals. (*Left*) FRQ and PER contain regions of similar length that display low folding propensity. These putative IDRs may adopt a rather compact conformation, potentially around FRH and CRYs, respectively. CK1, recruited through specific interaction domains, progressively phosphorylates, on a circadian time scale, low-affinity sites in the flexible IDRs. (*Right*) The increasing phosphorylation status becomes incompatible with the compact conformation of IDRs and favors open conformations, which may render the clock proteins inactive and prone to degradation (the dimerization domains of FRQ and PER2 are indicated by a red box, but only a monomeric clock protein is shown).

temperature or metabolic cues) (31, 33, 39, 53) but not be part of the timing mechanism per se. Novel experimental approaches based on this hypothesis need to clarify in subsequent work how the observed CK1-mediated progressive phosphorylation of FRQ and PER2 might mechanistically contribute to circadian time measurement in fungi and animals. Because of the putative functional redundancy of many phosphorylations, the approaches used to test this hypothesis must differ significantly from conventional experimental setups used to investigate the role of phosphorylation at specific sites. We have shown that CK1a and CK1δ phosphorylated FRQ and mPER2 by a similar mechanism, although these clock proteins display no sequence similarity. However, FRQ and PERs share several features that might be functionally relevant for circadian timing. FRQ and PERs are known to dimerize via a coiled-coil domain and double PAS domains, respectively (54, 55). Interestingly, both dimerization domains are flanked by segments that are similar in size. These regions have a low propensity for folding and are predicted to be largely disordered (Fig. 6*A* and *SI Appendix*, Fig. S5). Although the sequences of these putative intrinsically disordered regions (IDRs) are not conserved (ca. 24% similarity between

mammalian and *Drosophila* PERs and ca. 24% between PERs and FRQ), they are enriched in serine residues, which is characteristic for many disordered regions (56, 57). Remarkably, the IDRs of FRQ and PER2 contain a similarly large number of serine/threonine residues, 183 and 225, respectively. For FRQ, it is also known that more than half of such residues can be phosphorylated in vivo (45). Finally, FRQ recruits FRH via its C-terminal portion, and mammalian and *Drosophila* PERs recruit CRYs and TIM, respectively. FRH, CRYs, and TIM are not related, but they protect their respective interaction partner from rapid degradation in addition to their other clock-specific functions in the respective organism (for review, refs. 2–4).

FRQ and PER hyperphosphorylation appears to be governed by three factors (Fig. 6*B*): the binding dynamics and equilibrium of CK1 to FRQ (48) or mPER2, the access of phosphorylation sites in the putative IDRs of these clock proteins to the active site of the bound CK1 molecule, and the low affinity of CK1 for the majority of the unprimed phosphorylation sites in FRQ and PER. In vitro, the phosphorylation kinetics are in a circadian range, because CK1 targets predominantly low-affinity sites. Hence, CK1 binds to disordered clock

proteins such as FRQ and PER to form functionally equivalent, phospho-based modules that have the potential to act as a pacemaker measuring time on a circadian scale. Hyperphosphorylation of FRQ and mPER2 by CK1 could affect the overall or local conformation or compactness of the IDRs (Fig. 6*B*) (58–60). This could modulate interactions with binding partners and thereby determine the timing of FRQ or PER nuclear entry or influence the active lifetime of FRQ or PER complexes (6, 61–64). A change in compactness of IDRs could readily be triggered by a critical number of phosphorylated sites and be highly redundant with respect to the sites that are actually phosphorylated in a particular region of these proteins.

Interestingly, overexpression of CK1a and CK1δ shortened the circadian period length in *Neurospora* and T-REx-U2OS cells, respectively, indicating that CK1 was functionally limiting in both models. Furthermore, expression of the catalytically inactive CK1δ-K38R mutant in T-REx-U2OS cells lengthened and severely damped the circadian period. This dominant negative effect suggests that the mPER–CK1 binding equilibrium is a crucial determinant of the circadian period length. In agreement, it has been shown that mutations in FRQ's FCD1 that weaken the interaction with CK1a lengthen the circadian period (65).

In conclusion, evolutionarily conserved CK1 family members and their nonorthologous but architecturally similar clock protein clients, FRQ and mPER2, and potentially also other PERs form functionally equivalent, phospho-based modules that are in principle suited to measure time on the circadian scale. Our results support a model in which CK1 is recruited to FRQ and PERs, which have long, flexible IDRs containing ~200 low-affinity phosphorylation sites. These sites are slowly and steadily phosphorylated by the bound kinase, such that the phosphorylation state of the clock proteins is essentially proportional to the time elapsed since the start of the reaction. Theoretical considerations suggest that slow, random multiple phosphorylation has the potential to trigger delayed switch-like behavior that may be critical for circadian rhythm generation (66). It will be crucial to identify in subsequent work the mechanistic readout of this timing module. In addition to priming-independent phosphorylation, priming of specific sites and subsequent rapid priming-dependent phosphorylation of such

high-affinity sites by CK1 could relay external signals to reset and control the clock. Hence, CK1's ability to slowly phosphorylate low-affinity sites combined with its ability to rapidly phosphorylate primed sites make the kinase ideally suited to act on FRQ and PERs in the core pacemaker of circadian clocks. Acting solely within the negative feedback phase, this conserved timing module could be a major determinant of circadian period length and waveform, but it cannot account for the temporal dynamics of the full circadian cycle.

## Materials and Methods

**ChEF Assay.** The activity of CK1a and CK1δ at 20 °C was measured by $Mg^{2+}$ ChEF (*SI Appendix, SI Methods*).

**In Vitro Phosphorylation Assay and Quantification.** If not stated otherwise, phosphorylation was performed with 10 mM ATP, 8.3 nM recombinant FRQ, and 95 nM CK1a or 18 to 50 μg HEK lysate (with overexpressed mPER2) and 41.7 nM recombinant CK1δ, respectively. For phosphorylation of FRQ by WCL from yeast, total protein concentration was adjusted to 1.67 mg/mL. Autophosphorylation of CK1δ was performed with 100 nM recombinant kinase. Assay conditions are described in *SI Appendix, SI Methods*.

**Time Course Bioluminescence Measurements.** Bioluminescence of T-REx-U2OS cells expressing p*Bmal1-luc* and *Neurospora* strains expressing *frq-luc*PEST was measured with a plate reader (EnSpire from PerkinElmer) placed in a temperature-controlled incubator (CLF Plant Climatics E41L1C8) as described in *SI Appendix, SI Methods*.

Information on transfection and lysis of HEK293T cells, race tube assay, generation of stable U2OStx cell lines, construction of genomically modified *Neurospora crassa*, sodium dodecyl sulfate–polyacrylamide gel electrophoresis (SDS-PAGE), Western blotting, expression and purification of recombinant proteins, protein extraction from *S. cerevisiae*, cloning, culture conditions of clonal cell lines and *Neurospora* strains, dephosphorylation of CK1a, and nano differential scanning fluorimetry can be found in *SI Appendix, SI Methods*.

**Data Availability.** All study data are included in the article and/or supporting information.

1. M. Rosbash, The implications of multiple circadian clock origins. *PLoS Biol.* **7**, e62 (2009).
2. K. H. Cox, J. S. Takahashi, Circadian clock genes and the transcriptional architecture of the clock mechanism. *J. Mol. Endocrinol.* **63**, R93–R102 (2019).
3. A. Patke, M. W. Young, S. Axelrod, Molecular mechanisms and physiological importance of circadian rhythms. *Nat. Rev. Mol. Cell Biol.* **21**, 67–84 (2020).
4. J. C. Dunlap, J. J. Loros, Making time: Conservation of biological clocks from fungi to animals. *Microbiol. Spectr.* **5** (2017).
5. A. C. R. Diernfellner, M. Brunner, Phosphorylation timers in the Neurospora crassa circadian clock. *J. Mol. Biol.* **432**, 3449–3465 (2020).
6. C. L. Partch, Orchestration of circadian timing by macromolecular protein assemblies. *J. Mol. Biol.* **432**, 3426–3448 (2020).
7. J. Blau, M. W. Young, Cycling vrille expression is required for a functional Drosophila clock. *Cell* **99**, 661–671 (1999).
8. S. A. Cyran et al., vrille, Pdp1, and dClock form a second feedback loop in the Drosophila circadian clock. *Cell* **112**, 329–341 (2003).
9. N. R. Glossop et al., VRILLE feeds back to control circadian transcription of clock in the Drosophila circadian oscillator. *Neuron* **37**, 249–261 (2003).
10. N. Preitner et al., The orphan nuclear receptor REV-ERBalpha controls circadian transcription within the positive limb of the mammalian circadian oscillator. *Cell* **110**, 251–260 (2002).
11. G. Sancar et al., A global circadian repressor controls antiphasic expression of metabolic genes in Neurospora. *Mol. Cell* **44**, 687–697 (2011).
12. B. Kornmann, O. Schaad, H. Bujard, J. S. Takahashi, U. Schibler, System-driven and oscillator-dependent circadian transcription in mice with a conditionally active liver clock. *PLoS Biol.* **5**, e34 (2007).
13. C. Sancar, G. Sancar, N. Ha, F. Cesbron, M. Brunner, Dawn- and dusk-phased circadian transcription rhythms coordinate anabolic and catabolic functions in Neurospora. *BMC Biol.* **13**, 17 (2015).
14. J. K. Cheong, D. M. Virshup, Casein kinase 1: Complexity in the family. *Int. J. Biochem. Cell Biol.* **43**, 465–469 (2011).
15. P. R. Graves, P. J. Roach, Role of COOH-terminal phosphorylation in the regulation of casein kinase I delta. *J. Biol. Chem.* **270**, 21689–21694 (1995).
16. C. L. Dahlberg, E. Z. Nguyen, D. Goodlett, D. Kimelman, Interactions between Casein kinase Iepsilon (CKIepsilon) and two substrates from disparate signaling pathways reveal mechanisms for substrate-kinase specificity. *PLoS One* **4**, e4766 (2009).
17. P. Xu et al., Structure, regulation, and (patho-)physiological functions of the stress-induced protein kinase CK1 delta (CSNK1D). *Gene* **715**, 144005 (2019).
18. H. Flotow et al., Phosphate groups as substrate determinants for casein kinase I action. *J. Biol. Chem.* **265**, 14264–14269 (1990).
19. O. Marin et al., A noncanonical sequence phosphorylated by casein kinase 1 in beta-catenin may play a role in casein kinase 1 targeting of important signaling proteins. *Proc. Natl. Acad. Sci. U.S.A.* **100**, 10193–10200 (2003).
20. F. Kawakami, K. Suzuki, K. Ohtsuki, A novel consensus phosphorylation motif in sulfatide- and cholesterol-3-sulfate-binding protein substrates for CK1 in vitro. *Biol. Pharm. Bull.* **31**, 193–200 (2008).
21. H. Flotow, P. J. Roach, Role of acidic residues as substrate determinants for casein kinase I. *J. Biol. Chem.* **266**, 3724–3727 (1991).
22. R. M. Xu, G. Carmel, R. M. Sweet, X. Cheng, Crystal structure of casein kinase-1, a phosphate-directed protein kinase. *EMBO J.* **14**, 1015–1023 (1995).
23. K. L. Longenecker, P. J. Roach, T. D. Hurley, Three-dimensional structure of mammalian casein kinase I: Molecular basis for phosphate recognition. *J. Mol. Biol.* **257**, 618–631 (1996).
24. J. M. Philpott et al., Casein kinase 1 dynamics underlie substrate selectivity and the PER2 circadian phosphoswitch. *eLife* **9**, e52343 (2020).
25. P. L. Lowrey et al., Positional syntenic cloning and functional characterization of the mammalian circadian mutation tau. *Science* **288**, 483–492 (2000).
26. M. Görl et al., A PEST-like element in FREQUENCY determines the length of the circadian period in Neurospora crassa. *EMBO J.* **20**, 7074–7084 (2001).
27. Q. He et al., FWD1-mediated degradation of FREQUENCY in Neurospora establishes a conserved mechanism for circadian clock regulation. *EMBO J.* **22**, 4421–4430 (2003).

Marzoll et al.
Casein kinase 1 and disordered clock proteins form functionally equivalent, phospho-based circadian modules in fungi and mammals

PNAS | 9 of 10
https://doi.org/10.1073/pnas.2118286119

BIOCHEMISTRY

28. C. Querfurth et al., Circadian conformational change of the Neurospora clock protein FREQUENCY triggered by clustered hyperphosphorylation of a basic domain. *Mol. Cell* **43**, 713–722 (2011).

29. H. W. Ko, J. Jiang, I. Edery, Role for slimb in the degradation of Drosophila period protein phosphorylated by Doubletime. *Nature* **420**, 673–678 (2002).

30. B. Grima et al., The F-box protein slimb controls the levels of clock proteins period and timeless. *Nature* **420**, 178–182 (2002).

31. M. Zhou, J. K. Kim, G. W. Eng, D. B. Forger, D. M. Virshup, A Period2 phosphoswitch regulates and temperature compensates circadian period. *Mol. Cell* **60**, 77–88 (2015).

32. K. L. Toh et al., An hPer2 phosphorylation site mutation in familial advanced sleep phase syndrome. *Science* **291**, 1040–1043 (2001).

33. R. Narasimamurthy et al., CK1δ/ε protein kinase primes the PER2 circadian phosphoswitch. *Proc. Natl. Acad. Sci. U.S.A.* **115**, 5986–5991 (2018).

34. N. P. Shanware et al., Casein kinase 1-dependent phosphorylation of familial advanced sleep phase syndrome-associated residues controls PERIOD 2 stability. *J. Biol. Chem.* **286**, 12766–12774 (2011).

35. K. Vanselow et al., Differential effects of PER2 phosphorylation: Molecular basis for the human familial advanced sleep phase syndrome (FASPS). *Genes Dev.* **20**, 2660–2672 (2006).

36. Y. Xu et al., Modeling of a human circadian mutation yields insights into clock regulation by PER2. *Cell* **128**, 59–70 (2007).

37. E. J. Eide et al., Control of mammalian circadian rhythm by CKIepsilon-regulated proteasome-mediated PER2 degradation. *Mol. Cell. Biol.* **25**, 2795–2807 (2005).

38. Y. Isojima et al., CKIepsilon/delta-dependent phosphorylation is a temperature-insensitive, period-determining process in the mammalian circadian clock. *Proc. Natl. Acad. Sci. U.S.A.* **106**, 15744–15749 (2009).

39. S. Masuda et al., Mutation of a PER2 phosphodegron perturbs the circadian phosphoswitch. *Proc. Natl. Acad. Sci. U.S.A.* **117**, 10888–10896 (2020).

40. J. C. Chiu, H. W. Ko, I. Edery, NEMO/NLK phosphorylates PERIOD to initiate a time-delay phosphorylation circuit that sets circadian clock speed. *Cell* **145**, 357–370 (2011).

41. D. S. Garbe et al., Cooperative interaction between phosphorylation sites on PERIOD maintains circadian period in Drosophila. *PLoS Genet.* **9**, e1003749 (2013).

42. A. Cegielska, K. F. Gietzen, A. Rivers, D. M. Virshup, Autoinhibition of casein kinase I epsilon (CKI epsilon) is relieved by protein phosphatases and limited proteolysis. *J. Biol. Chem.* **273**, 1357–1364 (1998).

43. G. Guo et al., Autokinase activity of casein kinase 1 δ/ε governs the period of mammalian circadian rhythms. *J. Biol. Rhythms* **34**, 482–496 (2019).

44. Y. Shinohara et al., Temperature-sensitive substrate and product binding underlie temperature-compensated phosphorylation in the clock. *Mol. Cell* **67**, 783–798.e20 (2017).

45. C. L. Baker, A. N. Kettenbach, J. J. Loros, S. A. Gerber, J. C. Dunlap, Quantitative proteomics reveals a dynamic interactome and phase-specific phosphorylation in the Neurospora circadian clock. *Mol. Cell* **34**, 354–363 (2009).

46. C. T. Tang et al., Setting the pace of the Neurospora circadian clock by multiple independent FRQ phosphorylation events. *Proc. Natl. Acad. Sci. U.S.A.* **106**, 10722–10727 (2009).

47. N. Y. Garceau, Y. Liu, J. J. Loros, J. C. Dunlap, Alternative initiation of translation and time-specific phosphorylation yield multiple forms of the essential clock protein FREQUENCY. *Cell* **89**, 469–476 (1997).

48. L. Lauinger, A. Diernfellner, S. Falk, M. Brunner, The RNA helicase FRH is an ATP-dependent regulator of CK1a in the circadian clock of Neurospora crassa. *Nat. Commun.* **5**, 3598 (2014).

49. R. Narasimamurthy, D. M. Virshup, The phosphorylation switch that regulates ticking of the circadian clock. *Mol. Cell* **81**, 1133–1146 (2021).

50. H. Lee, R. Chen, Y. Lee, S. Yoo, C. Lee, Essential roles of CKIdelta and CKIepsilon in the mammalian circadian clock. *Proc. Natl. Acad. Sci. U.S.A.* **106**, 21359–21364 (2009).

51. S. A. Brown et al., PERIOD1-associated proteins modulate the negative limb of the mammalian circadian oscillator. *Science* **308**, 693–696 (2005).

52. M. J. Muskus, F. Preuss, J. Y. Fan, E. S. Bjes, J. L. Price, Drosophila DBT lacking protein kinase activity produces long-period and arrhythmic circadian behavioral and molecular rhythms. *Mol. Cell. Biol.* **27**, 8049–8064 (2007).

53. A. Mehra et al., A role for casein kinase 2 in the mechanism underlying circadian temperature compensation. *Cell* **137**, 749–760 (2009).

54. P. Cheng, Y. Yang, C. Heintzen, Y. Liu, Coiled-coil domain-mediated FRQ-FRQ interaction is essential for its circadian clock function in Neurospora. *EMBO J.* **20**, 101–108 (2001).

55. S. Hennig et al., Structural and functional analyses of PAS domain interactions of the clock proteins Drosophila PERIOD and mouse PERIOD2. *PLoS Biol.* **7**, e94 (2009).

56. V. N. Uversky, Proteins without unique 3D structures: Biotechnological applications of intrinsically unstable/disordered proteins. *Biotechnol. J.* **10**, 356–366 (2015).

57. V. N. Uversky, Intrinsically disordered proteins and their "mysterious" (meta)physics. *Front. Phys.* **7**, 10 (2019).

58. S. Müller-Späth et al., From the cover: Charge interactions can dominate the dimensions of intrinsically disordered proteins. *Proc. Natl. Acad. Sci. U.S.A.* **107**, 14609–14614 (2010).

59. P. E. Wright, H. J. Dyson, Intrinsically disordered proteins in cellular signalling and regulation. *Nat. Rev. Mol. Cell Biol.* **16**, 18–29 (2015).

60. M. E. Fealey, B. P. Binder, V. N. Uversky, A. Hinderliter, D. D. Thomas, Structural Impact of phosphorylation and dielectric constant variation on synaptotagmin's IDR. *Biophys. J.* **114**, 550–561 (2018).

61. A. Takano, Y. Isojima, K. Nagai, Identification of mPer1 phosphorylation sites responsible for the nuclear entry. *J. Biol. Chem.* **279**, 32578–32585 (2004).

62. J. S. Takahashi, Transcriptional architecture of the mammalian circadian clock. *Nat. Rev. Genet.* **18**, 164–179 (2017).

63. V. H. Lam et al., CK1α collaborates with DOUBLETIME to regulate PERIOD function in the *Drosophila* circadian clock. *J. Neurosci.* **38**, 10631–10643 (2018).

64. C. Lee, J. P. Etchegaray, F. R. Cagampang, A. S. Loudon, S. M. Reppert, Posttranslational mechanisms regulate the mammalian circadian clock. *Cell* **107**, 855–867 (2001).

65. X. Liu et al., FRQ-CK1 interaction determines the period of circadian rhythms in Neurospora. *Nat. Commun.* **10**, 4352 (2019).

66. A. Upadhyay, D. Marzoll, A. Diernfellner, M. Brunner, H. Herzel, Multiple random phosphorylations in clock proteins provide long delays and switches. *Sci. Rep.* **10**, 22224 (2020).

67. R. Gautier, D. Douguet, B. Antonny, G. Drin, HELIQUEST: A web server to screen sequences with specific α-helical properties. *Bioinformatics* **24**, 2101–2102 (2008).

68. F. Cesbron, M. Oehler, N. Ha, G. Sancar, M. Brunner, Transcriptional refractoriness is dependent on core promoter architecture. *Nat. Commun.* **6**, 6753 (2015).

69. F. Cesbron, M. Brunner, A. C. Diernfellner, Light-dependent and circadian transcription dynamics in vivo recorded with a destabilized luciferase reporter in Neurospora. *PLoS One* **8**, e83660 (2013).